Shelling and Sinking Graphs on the Sphere

Anonymous author(s)
Anonymous affiliation(s)

Abstract

We describe a promising approach to efficiently morph spherical graphs, extending earlier approaches of Awartani and Henderson [*Trans. AMS* 1987] and Kobourov and Landis [*JGAA* 2006]. Specifically, we describe two methods to morph shortest-path triangulations of the sphere by moving their vertices along longitudes into the southern hemisphere; we call a triangulation *sinkable* if such a morph exists. Our first method generalizes a longitudinal shelling construction of Awartani and Henderson; a triangulation is sinkable if a specific orientation of its dual graph is acyclic. We describe a simple polynomial-time algorithm to find a longitudinal shellable rotation of a given spherical triangulation, if one exists; we also construct a spherical triangulation that has no longitudinally shellable rotation. Our second method is based on a linear-programming characterization of sinkability. By identifying its optimal basis, we show that this linear program can be solved in $O(n^{\omega/2})$ time, where ω is the matrix-multiplication exponent, assuming the underlying linear system is non-singular. Finally, we pose several conjectures and describe experimental results that support them.

2012 ACM Subject Classification Theory of computation → Computational geometry

Keywords and phrases morphing, planar graphs, spherical graph drawing, longitudinal shelling

1 Introduction

A *morph* between two planar straight-line graphs is a continuous deformation from one to the other, such that all edges in all intermediate graphs are straight line segments. Planar graph morphing has many applications in graphics, animation, visualization, and geometric modeling, as well as connections to fundamental questions in low-dimensional topology.

There are two state-of-the-art approaches for morphing planar graphs. The first is the barycentric interpolation method of Floater, Gotsman, and Surazhsky [35, 38, 41, 72–74], which is based on an extension by Floater [36, 37] of Tutte's classical spring-embedding theorem [76]. These algorithms compute an implicit representation of a smooth morph, any intermediate stage of which can be constructed in $O(n^{\omega/2}) = O(n^{1.1864})$ time, where $\omega < 2.3728$ is the matrix-multiplication exponent. The second method combines an edge-collapsing strategy originally proposed by Cairns [12,13,47,75] with more recent algorithms for convex hierarchical graph drawing [18, 21, 48, 52, 53]. This method has led to several efficient algorithms for constructing explicit representations of piecewise-linear morphs [2, 52, 53]. The fastest of these algorithms, due to Klemz [53], computes a morph consisting of $O(n)$ stages in $O(n^2)$ time, where in each stage, all vertices move along parallel lines at constant speeds. A recent algorithm of Erickson and Lin computes explicit piecewise-linear morphs using barycentric interpolation in $O(n^{1+\omega/2})$ time [33]. Algorithms are also known for several variants [5, 6, 56].

Both planar morphing approaches have recently been generalized to geodesic graphs on the flat torus [19, 33, 58], and very recently, Luo, Wu, and Zhu generalized the barycentric interpolation method to arbitrary negative-curvature surfaces of higher genus [59, 60].

1.1 What about the sphere?

In light of the long history of results for morphing planar graphs and their generalizations to higher-genus surface, it is surprising how little is known about morphing graphs on the

sphere. Although embeddings on the sphere are topologically equivalent to embeddings in the plane, the different geometries of the two surfaces induce significantly different behavior.

In 1944, Cairns [13] proved that any two isomorphic shortest-path triangulations of the sphere are connected by a continuous family of shortest-path triangulations, using essentially the same edge-contraction strategy that he used for planar triangulations (but with more complex case analysis). A direct translation of Cairns's spherical morphing proof leads to an exponential-time algorithm; unlike his planar result, this is still the fastest algorithm known. In fact, as far as we are aware, this is the *only* algorithm known for morphing arbitrary spherical triangulations.

Morphing algorithms are known for a few special cases of sphere graphs, almost all by moving vertices along longitudes into the southern hemisphere, projecting the resulting southern embedding into the plane, and applying a planar morphing algorithm. Awartani and Henderson [4] describe an algorithm to morph triangulations that satisfy a certain *shelling* condition using this strategy. They also prove that any triangulation with a *longitudinal seam*, meaning there is a longitude that does not cross the interior of any edge, satisfies their shelling condition. (We study Awartani and Henderson's shelling condition in more detail in Section 3.) Kobourov and Landis [54] describe an algorithm to morph between *Delaunay* triangulations via longitudinal morphs; their algorithm easily generalizes to *coherent* triangulations, which are central projections of arbitrary convex polyhedra. The same method is also implicit in Richter-Gebert's proof [63, Theorem 13.3.3] of classical theorems of Eberhard [30] and Steinitz [66] describing morphs between isomorphic convex polyhedra.

We call a sphere triangulation ***sinkable*** if it can be morphed along longitudes into the southern hemisphere. Awartani and Henderson [4] describe an example of an unsinkable triangulation; it is not possible to move the vertices of their triangulation into the southern hemisphere without inverting at least one face. The simplest examples of unsinkable triangulation are the central projections of sufficiently twisted *Schönhardt polyhedra* [64]; see Figure 1.1. (Supnick proved that Schönhardt triangulations are the simplest non-coherent triangulations [70, 71]; our algorithm in Section 5 can be used to determine which Schönhardt triangulations are unsinkable.)

1.2 Our Results

In this paper, we describe a promising approach to efficiently morph shortest-path embeddings of graphs on the sphere, extending the previous results of Awartani and Henderson [4] and Kobourov and Landis [54]. At a high level, we propose finding suitable rotations of the source and target embeddings and pushing both embeddings into the southern hemisphere along longitudes, thereby reducing to a planar morphing problem. We emphasize that we do *not* develop this strategy into a complete algorithm; the existence of an efficient spherical morphing algorithm remains an open problem.

We begin in Section 2 by reviewing relevant definitions and proving some preliminary results. In particular, we describe our proposed morphing strategy in detail. We also show that a triangulation Γ is sinkable if and only if there is an isomorphic *weak* triangulation Γ' (that is, a triangulation with degenerate faces) in the southern hemisphere, whose vertices are on the same longitudes.

In Section 3, we formally define the *longitudinal shelling* condition introduced by Awartani and Henderson and provide several combinatorial characterizations, each of which can be tested in $O(n)$ time. We also reiterate Awartani and Henderson's proof that every longitudinally shellable triangulations is sinkable.

In Section 4, we present an algorithm that either finds a rotation of a given sphere

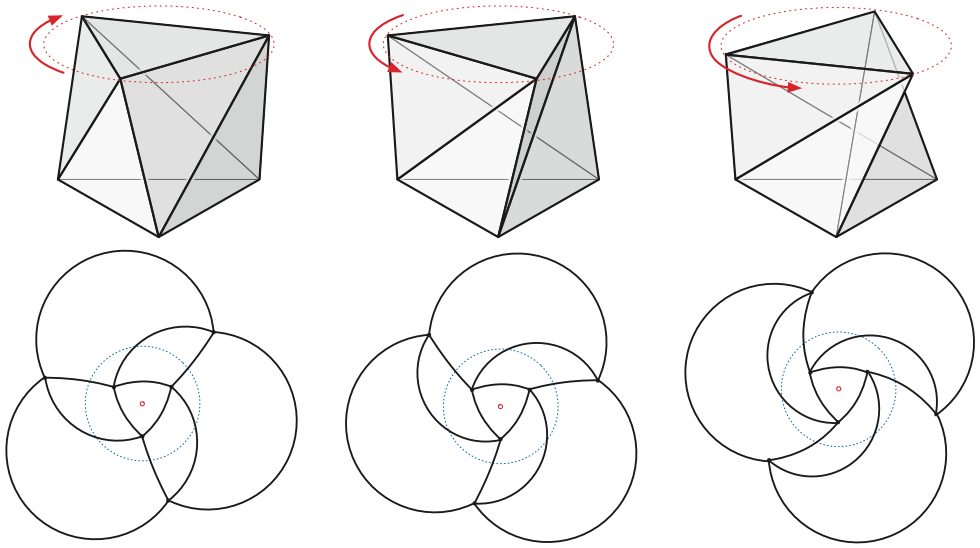

(a) (b) (c)

Figure 1.1 Three Schönhardt polyhedra and stereographic projections of the corresponding spherical triangulations. Depending on the twisting angle, these triangulations are (a) coherent and therefore longitudinally shellable, (b) sinkable but not longitudinally shellable, or (c) not sinkable.

triangulation Γ that is longitudinally shellable, or reports correctly that no such rotation exists, in $O(n^{5/2}\log^3 n)$ time. Our algorithm searches each of the $O(n^2)$ cells in the arrangement of great circles determined by the edges of Γ, using a dynamic reachability data structure of Diks and Sankowski [27]. Finally, we construct a spherical triangulation that has no longitudinally shellable rotation.

In Section 5, we describe an efficient algorithm to determine whether a given sphere triangulation is *sinkable*. First we report a straightforward equivalence between sinkability and the feasibility of a certain linear program with $O(n)$ variables and constraints. By identifying the optimal basis for this linear program, we show that it can be solved in $O(n^{\omega/2})$ time, assuming the underlying linear system is non-singular.

Due to space constraints, we defer proofs of several lemmas to Appendix A.

As a tool for building intuition, we implemented a suite of algorithms to construct sphere triangulations, test for shellability and sinkability, construct Awartani-Henderson embeddings, and visualize longitudinal morphs. In Appendix B, we present results of some lightweight experiments with "ugly" spherical triangulations, which suggest that "in practice", one can find a shellable rotation by testing a small constant number of random rotations.

Finally, we conclude in Appendix C by presenting several open problems for further research, including several conjectures suggested by our experimental results.

2 Background and Preliminary Results

2.1 Cartography

We consider drawings of graphs on the unit sphere $S^2 = \{(x, y, x) \mid x^y + 2 + z^2 = 1\}$. The ***north pole*** is the point $(0, 0, 1)$; the ***south pole*** is the point $(0, 0, -1)$; the ***equator*** is the intersection of the unit sphere with the plane $z = 0$. A ***longitude*** is a great-circular arc

whose endpoints are the north and south poles. Every point except the poles lies on a unique longitude.

Throughout the paper, we fix an arbitrary maximal simple planar graph G with $n \geq 4$ vertices, arbitrarily indexed from 1 to n. An ***embedding*** of G on the sphere is an injective map from G to S^2, or less formally, a drawing of G where edges intersect only at their shared endpoints. Classical theorems of Steinitz [43, 65, 66] and Whitney [10, 77] imply that G has a unique embedding on the sphere, up to homeomorphism, in which every edge is a shortest path between its vertices. A ***face*** of G is a face in this essentially unique embedding. We sometimes identify each face as a triple (i, j, k) of vertices (or their indices) in counterclockwise order around its interior.

Unless explicitly indicated otherwise, we consider only ***generic shortest-path*** triangulations, meaning (1) every edge is a great-circular arc with length less than π; (2) no great circle contains more than two vertices, and (3) no great circle through the poles contains more than one vertex. Condition (3) implies that vertices lie on distinct longitudes.

Every generic shortest-path triangulation has a unique ***north face*** that contains the north pole in its interior and a unique ***south face*** that contains the south pole in its interior. The remaining ***non-polar*** faces are of two types: An ***up-face*** has one vertex (called its ***apex***) that is directly north of its opposite edge (called its ***base***); symmetrically, a ***down-face*** has one vertex (its apex) directly south of its opposite edge (its base). The ***sides*** of a non-polar face f are the edges of f incident to the apex of f. The faces immediately north and south of any vertex i are respectively denoted $f_{\mathsf{above}}(i)$ and $f_{\mathsf{below}}(i)$. For each vertex i, $f_{\mathsf{above}}(i)$ is either the north face or a down-face, and $f_{\mathsf{below}}(i)$ is either the south face or an up-face.

A face of a (generic) triangulation is ***everted*** if it has area greater than 2π, or equivalently, if it contains an open hemisphere, or equivalently, if it contains a pair of antipodal points. Every triangulation contains at most one everted face. We call a triangulation ***full*** if no face is everted, and ***southern*** if its north face is everted but not its south face.

We call any connected region R on the sphere ***θ-monotone*** if every longitude is either disjoint from R or has connected intersection with R.

2.2 Coordinates

Throughout the paper, we represent spherical triangulations *implicitly* as projections of certain polyhedra onto the unit sphere. Specifically, we represent each vertex using signed homogeneous coordinates [67–69]—for any scalar $\lambda > 0$, the coordinate vectors (x, y, z) and $(\lambda x, \lambda y, \lambda z)$ represent the same point on the sphere. We can freely rescale the vertices, each independently, without changing the underlying spherical triangulation; although it is never actually necessary, this rescaling is sometimes convenient for purposes of discussion and intuition. For example, we can implicitly interpret any southern triangulation as a *planar* triangulation via gnomonic projection, by scaling vertices onto the tangent plane $z = -1$; Awartani and Henderson [4] analyze longitudinal morphing (defined below) by implicitly scaling vertices onto the unit cylinder $x^2 + y^2 = 1$.

Every full triangulation is the projection of a *star-shaped* polyhedron whose kernel contains the origin. Every non-full triangulation is the projection of a polyhedron that is star-shaped except for one facet.

2.3 Longitudinal Morphing

Two embeddings $\Gamma_0 \colon G \to S^2$ and $\Gamma_1 \colon G \to S^2$ are ***isomorphic*** if they define the same rotation system, or equivalently, if there is an orientation-preserving homeomorphism $H \colon S^2 \to S^2$

such that $\Gamma_1 = h \circ \Gamma_0$. Two isomorphic embeddings are ***θ-equivalent*** if each vertex lies on the same longitude in both embeddings.

A ***homotopy*** between two embeddings $\Gamma_0 \colon G \to S^2$ and $\Gamma_1 \colon G \to S^2$ is a continuous function $H \colon [0,1] \times G \to S^2$ such that $H(0,\cdot) = \Gamma_0$ and $H(1,\cdot) = \Gamma_1$. Any pair of isomorphic maps Γ_0 and Γ_1 are connected by an ***isotopy***, which is a homotopy H such that every intermediate drawing $\Gamma_t = H(t,\cdot)$ is an embedding. A ***morph*** is an isotopy in which the edges of every intermediate embedding Γ_t are shortest paths. Finally, a ***longitudinal morph*** is a morph in which vertices move only along their longitudes.

▶ **Lemma 2.1.** *Any two θ-equivalent triangulations are connected by a longitudinal morph.*

Proof sketch. Let Γ_0 and Γ_1 be two θ-equivalent triangulations. Without loss of generality (by scaling if necessary), each vertex has the same x- and y-coordinates in both embeddings. We define a longitudinal morph by linearly interpolating the z-coordinates of the vertices. The signed volume spanned by the vertices of any face is a linear function of the interpolation parameter t. Each non-polar face has the same orientation in Γ_0 and Γ_1, and therefore in every intermediate embedding. (See Appendix A for a more detailed proof.) ◀

We extend this lemma slightly by considering ***weak triangulations***, which are drawings of G that may include degenerate faces, but no inverted faces or crossing edges [1,39]. A weak embedding Γ_1 is θ-equivalent to a triangulation Γ_0 if vertices lie on the same longitudes in Γ_0 and Γ_1 and every non-degenerate non-polar face of Γ_i has the same orientation as the corresponding face of Γ_0. The following lemma is immediate:

▶ **Lemma 2.2.** *Any embedding Γ_0 and any weak embedding Γ_1 that is longitudinally equivalent to Γ_0 are connected by a homotopy H, such that for any $0 < \varepsilon < 1$, the restriction of H to the interval $[0, 1-\varepsilon]$ is a longitudinal morph.*

2.4 Morphing Strategy

We propose a strategy for morphing between isomorphic shortest-path triangulations on the sphere that slightly generalizes strategies previously used by Awartani and Henderson [4] and Kobourov and Landis [54]. We call a triangulation ***sinkable*** if it can be longitudinally morphed to a θ-equivalent triangulation with all vertices below the equator. Our strategy rests on the following (admittedly optimistic) conjecture:

▶ **Conjecture 2.3.** *Every shortest-path triangulation of the sphere has a sinkable rotation.*

Conjecture 2.3 implies that one can morph any triangulation Γ_0 into any isotopic target triangulation Γ_1 through an intermediate coherent triangulation $\Gamma_{1/2}$. Steinitz's theorem [43, 65, 66] implies that a coherent embedding $\Gamma_{1/2}$ of G exists. Given any coherent triangulation, we can project its underlying convex polyhedron to a triangulation in the plane (following Cauchy's proof of Euler's formula [15]) and then centrally project back to the southern hemisphere to obtain a θ-equivalent southern triangulation. It follows that *every* rotation of a coherent triangulation is sinkable.

We construct a morph from Γ_0 to $\Gamma_{1/2}$ as follows. First, we rotate Γ_0 so that the resulting map Γ_ε is sinkable (as guaranteed by Conjecture 2.3) and then longitudinally morph Γ_ε to a southern triangulation $\Gamma_{2\varepsilon}$. Similarly, we rotate $\Gamma_{1/2}$ so that the resulting map $\Gamma_{1/2-\varepsilon}$ has the same north face as Γ_ε and $\Gamma_{2\varepsilon}$, and then longitudinally morph $\Gamma_{1/2-\varepsilon}$ to a southern triangulation $\Gamma_{1/2-2\varepsilon}$. Gnomonic projection maps both $\Gamma_{2\varepsilon}$ and $\Gamma_{1/2-2\varepsilon}$ to isomorphic straight-line triangulations in the plane $z = -1$, each with the same triangular

outer face. We can construct a morph between these planar triangulations using any of several algorithms [2, 8, 12, 33, 38, 45, 53]; projecting this planar morph back to the sphere yields a spherical morph from $\Gamma_{2\varepsilon}$ to $\Gamma_{1/2-2\varepsilon}$. Our final morph is the concatenation of the rotation and longitudinal morph $\Gamma_0 \rightsquigarrow \Gamma_{2\varepsilon}$, the lifted planar morph $\Gamma_{2\varepsilon} \rightsquigarrow \Gamma_{1/2-2\varepsilon}$, and the reverse of the rotation and longitudinal morph $\Gamma_{1/2} \rightsquigarrow \Gamma_{1/2-2\varepsilon}$. See Figure 2.1 for an example (without the initial and final rotations).

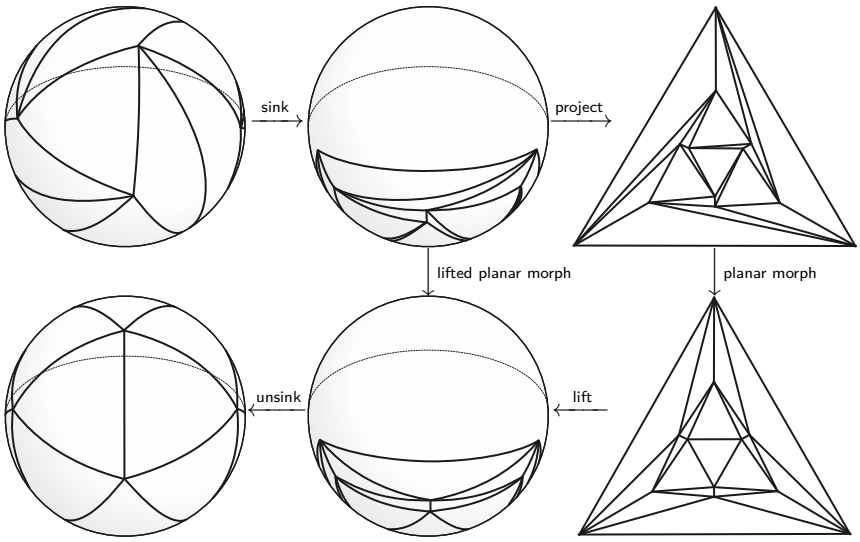

Figure 2.1 Morphing a six-beaked shaddock [28, 50] into a regular icosahedron; compare with Kobourov and Landis [54, Figure 1].

We construct a morph $\Gamma_1 \rightsquigarrow \Gamma_{1/2}$ using the same strategy. The final morph $\Gamma_0 \rightsquigarrow \Gamma_1$ is the concatenation of $\Gamma_0 \rightsquigarrow \Gamma_{1/2}$ and the reverse of $\Gamma_1 \rightsquigarrow \Gamma_{1/2}$.

3 Longitudinal Shelling

A ***shelling*** of a spherical triangulation Γ is an ordering $f_1, f_2, \ldots, f_{2n-4}$ of the faces of Γ such that the union of any prefix $U_k = \bigcup_{i \le k} f_i$ is either empty ($k = 0$), the entire sphere ($k = 2n - 4$), or a topological disk. We call a shelling ***longitudinal*** if every disk U_k is θ-monotone.

Bruggesser and Mani's line shelling [11] implies that every *coherent* triangulation is longitudinally shellable. Awartani and Henderson [4] proved that a triangulation is longitudinally shellable if it has a *longitudinal seam*, that is, a longitude ℓ such that for any edge e, the intersection $\ell \cap e$ is either empty, an endpoint of e, or the entire edge e.

3.1 Characterization

We characterize the shellability of Γ in terms of three directed graphs; see Figure 3.1.

- The directed dual graph $\Gamma^{\downarrow}$ contains a directed edge from face f_i to face f_j if and only if f_i and f_j share an edge in Γ, and some point in f_i is due north (on the same longitude) of some point in f_j. The north face of Γ has out-degree 3 in $\Gamma^{\downarrow}$; each down-face has in-degree 1 and out-degree 2; each up-face has in-degree 2 and out-degree 1, and the south face has in-degree 3.

- The oriented primal graph $\boldsymbol{\Gamma^{\rightarrow}}$ is the directed dual of $\Gamma^{\downarrow}$. For every undirected edge ij of Γ, the graph $\Gamma^{\rightarrow}$ contains the directed edge $i{\rightarrow}j$ if and only if vertex j is east of vertex i, or more formally, if the determinant

$$\det \begin{pmatrix} 0 & 0 & 1 \\ x_i & y_i & z_i \\ x_j & y_j & z_j \end{pmatrix} = \det \begin{pmatrix} x_i & y_i \\ x_j & y_j \end{pmatrix}$$

  is positive, where (x_i, y_i, z_i) is the coordinate vector for vertex i.
- Finally, $\boldsymbol{\Gamma^{\searrow\!\swarrow}}$ is a directed proper subgraph of Γ whose edges are the sides of each down-face, each directed toward its apex.

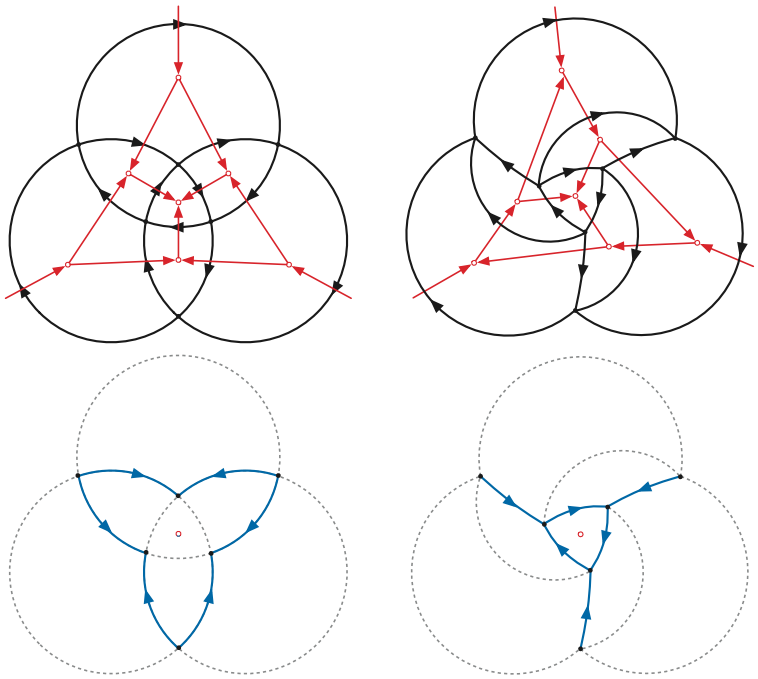

Figure 3.1 Directed graphs $\Gamma^{\downarrow}$ (red straight edges), $\Gamma^{\rightarrow}$ (black curved edges), and $\Gamma^{\searrow\!\swarrow}$ (blue, second row) for the Platonic octahedral triangulation (which is longitudinally shellable) and a Schönhardt triangulation (which is not).

We defer the proof of the following lemma to Appendix A.

▶ **Lemma 3.1.** *For every generic shortest-path triangulation Γ, the following conditions are equivalent:*

(a) *Γ is longitudinally shellable.*
(b) *$\Gamma^{\downarrow}$ is acyclic.*
(c) *$\Gamma^{\rightarrow}$ is strongly connected.*
(d) *$\Gamma^{\rightarrow}$ contains directed paths from f_{north} to f_{south} and from f_{south} to f_{north}.*
(e) *$\Gamma^{\searrow\!\swarrow}$ is acyclic.*

Each of the conditions (b), (c), (d), and (e) can be tested in $O(n)$ time using textbook graph algorithms.

Awartani and Henderson [4] explicitly consider spherical triangulations with vertical edges. It is straightforward to extend Lemma 3.1 to such triangulations by *including* both

orientations of vertical edges in $\Gamma^{\rightarrow}$, *excluding* both orientations of their dual edges from $\Gamma^{\downarrow}$, and *excluding* both orientations of vertical edges from $\Gamma^{\searrow\swarrow}$. With this extension, Lemma 3.1 immediately implies a key result of Awartani and Henderson:

▶ **Corollary 3.2** (Awartani and Henderson [4]). *If Γ has a longitudinal seam, then Γ is longitudinally shellable.*

Proof. Suppose longitude ℓ does not cross any edge of Γ. Then Γ contains an undirected path of vertical edges along ℓ between the north and south faces. It follows that $\Gamma^{\rightarrow}$ contains *directed* paths along ℓ from each polar face to the other. We conclude that Γ meets condition (d) of Lemma 3.1. ◀

3.2 The Awartani–Henderson Embedding

▶ **Theorem 3.3** (Awartani and Henderson [4]). *Every longitudinally shellable triangulation of the sphere is sinkable. Moreover, given any longitudinally shellable triangulation Γ, we can compute a longitudinal morph from Γ to a southern triangulation in $O(n)$ time.*

Proof sketch. Consider the vertices of Γ in any topological order of $\Gamma^{\searrow\swarrow}$. (This is an example of a *canonical order* for Γ [14, 26].) The first three vertices lie on the north face and thus can be placed anywhere below the equator on their respective longitudes; then for each later vertex i, we make z'_i as large as possible, such that no face induced by vertices 1 through i (except the north face) is inverted. (We give a more detailed proof, more closely following Awartani and Henderson [4], in Appendix A.) ◀

4 Shellable Rotations

When a given triangulation Γ is not longitudinally shellable, we can still apply our morphing strategy if we can find a rotation of Γ that is rotationally shellable. In this section, we describe an efficient algorithm that either finds such a rotation or correctly report that no such rotation exists. Our experimental results (described in Appendix B) suggest that even for triangulations with many long skinny triangles, a significant fraction of rotations are shellable, so it suffices to consider a small number of random rotations. In fact, *none* of the thousands of random triangulations we generated had no shellable rotation. Nevertheless, in Section 4.2, we construct a triangulation with no shellable rotations.

4.1 Finding a Shelling Direction

Instead of considering different rotations of Γ, it is convenient to keep Γ fixed and consider different locations for the north pole. We call a unit vector p a ***shelling direction*** for Γ if any (and therefore every) rotation of the sphere that takes p to the standard north pole $(0, 0, 1)$ also takes Γ to a longitudinally shellable triangulation. We similarly define the directed graphs $\Gamma^{\downarrow}(p)$ and $\Gamma^{\rightarrow}(p)$ and $\Gamma^{\searrow\swarrow}(p)$. For example, for any unit vector $p = (x, y, z)$, the graph $\Gamma^{\rightarrow}(p)$ contains the edge $i{\rightarrow}j$ if and only if

$$\mathrm{vol}(p, i, j) := \det \begin{pmatrix} x & y & z \\ x_i & y_i & z_i \\ x_j & y_j & z_j \end{pmatrix} > 0,$$

and p is a shelling direction for Γ if and only if the graphs $\Gamma^{\downarrow}(p)$ and $\Gamma^{\searrow\swarrow}(p)$ are acyclic.

▶ **Theorem 4.1.** *Given any shortest-path triangulation Γ on the sphere, we can either compute a shelling direction for Γ or report correctly that no such direction exists, in $O(n^{2.5}\log^3 n)$ time.*

Proof. Each edge ij in Γ lies on a unique great circle; let $\mathcal{A}(\Gamma)$ denote the arrangement of all $3n-6$ such great circles. For any two unit vectors p and q, the graphs $\Gamma^{\rightarrow}(p)$ and $\Gamma^{\rightarrow}(q)$ are identical if and only if p and q lie in the same cell of $\mathcal{A}(\Gamma)$. Thus, for any cell C, we can write $\Gamma^{\rightarrow}(C)$ to denote the graph $\Gamma^{\rightarrow}(p)$ for any $p \in C$. If C and C' are adjacent two-dimensional cells of $\mathcal{A}(\Gamma)$, then $\Gamma^{\rightarrow}(C)$ and $\Gamma^{\rightarrow}(C')$ differ in the direction of exactly one edge.

We can find a shelling direction for Γ in $O(n^3)$ time by constructing the great-circle arrangement $\mathcal{A}(\Gamma)$, and then for each two-dimensional cell c, check whether $\Gamma^{\rightarrow}(c)$ is strongly connected. (This arrangement is centrally symmetric, and the gnomonic projection of either hemisphere to any tangent plane is an arrangement of *lines*. Thus, we can use any classical algorithm to construct line arrangements [20, 31, 32] instead of more sophisticated algorithms to construct arrangements of more general circles on spheres [16, 17].)

We can speed up this naive algorithm using a data structure of Diks and Sankowski for reachability queries in dynamic directed plane graphs [27]. Diks and Sankowski's data structure maintains a directed planar graph with a fixed embedding, supports edge insertions and deletions that do not change the embedding in $O(\sqrt{n}\log^3 n)$ time, and supports queries of the form "Is there a directed path from vertex i to vertex j?" in $O(\sqrt{n}\log^2 n)$ time.

To use this data structure, we traverse the dual graph of the arrangement $\mathcal{A}(\Gamma)$. At each two-dimensional cell C, we perform two reachability queries in $\Gamma^{\rightarrow}(C)$ between the two polar faces. If both reachability queries succeed, then by Lemma 3.1(d), cell c contains a shelling direction. When we move from a cell C to a neighboring cell C', we delete one edge and insert its reversal. Altogether, we perform $O(n^2)$ queries and $O(n^2)$ updates in the worst case. ◀

4.2 A Totally Unshellable Triangulation

For any directed cycle γ^* of darts in the undirected dual graph Γ^*, we define the ***polar region $P(\gamma^*)$*** to be the set of all north poles p such that the directed dual graph $\Gamma^{\downarrow}(p)$ contains every dart in γ^*. A unit vector p is a shelling direction for Γ if and only if $p \notin P(\gamma^*)$ for *every* directed dual cycle γ^*.

▶ **Lemma 4.2.** *For every directed cycle γ^* of darts in the dual graph Γ^*, the corresponding polar region $P(\gamma^*)$ is the interior of a convex spherical polygon, that is, the intersection of S^2 with a (possibly empty) open convex polyhedral cone.*

Proof. Let $i{\rightarrow}j$ be any dart in Γ, and let f and g be the faces incident to $i{\rightarrow}j$ on the left and right, respectively. The directed graph $\Gamma^{\downarrow}(p)$ contains the edge $f{\rightarrow}g$ if and only if the north pole p lies to the left of $i{\rightarrow}j$, or equivalently, if $\mathrm{vol}(p, i, j) > 0$. The set of all points p satisfying this inequality is an open hemisphere $H(f{\rightarrow}g)$. Finally, the polar region $P(\gamma^*)$ of any dual cycle γ^* is the intersection of $H(f{\rightarrow}g)$ over all $f{\rightarrow}g \in \gamma^*$. ◀

A ***rotor*** is the subset of faces of in Γ dual to any directed cycle γ^* in the undirected dual graph Γ^*. We sketch the construction of a triangulation Γ containing a small number of rotors, whose polar regions cover the entire sphere. We describe our construction in terms of an arbitrary sufficiently small angular parameter $\varepsilon > 0$; in practice, it suffices to set $\varepsilon \approx 1°$.

First we define a simple *equatorial rotor*, which triangulates a belt of width $O(\varepsilon^2)$ around a great circle using $O(1/\varepsilon)$ isosceles triangles with aspect ratio $O(\varepsilon)$ and with all edges at angle $O(\varepsilon)$ from the great circle. The triangulation edges are consistently oriented so that

for any north pole p sufficiently far from the rotor, the rotor defines a cycle in the directed dual graph $\Gamma^{\downarrow}(p)$. The polar region of (one orientation of) the rotor is a convex spherical polygon whose boundary has Hausdorff distance $O(\varepsilon)$ from the rotor itself. In particular, in the limit as ε approaches zero, this polar region approaches an open hemisphere.

Figure 4.1 Local structure of an equatorial rotor.

Our unshellable triangulation contains four modified equatorial rotors, whose central great circles are parallel to the faces of a regular tetrahedron. Let Q denote the arrangement of these four great circles; Q is the central projection of an inscribed semi-regular cuboctahedron; see Figure 4.2. Each pair of great circles meets at an angle of $\arccos(1/3) \approx 70.529°$.

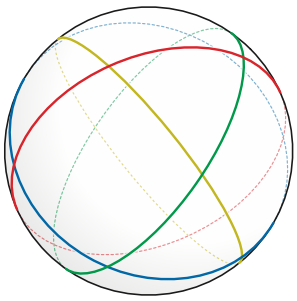

Figure 4.2 Four great circles defining a spherical cuboctahedron.

At each vertex of Q, we modify the two equatorial rotors by introducing a *crossing gadget*, illustrated in Figure 4.3(a). Overall the gadget resembles a rhombus with diameter $O(\varepsilon)$ whose edges are parallel to the great circles defining the rotors. Each of the equatorial rotors is broken and offset by $O(\varepsilon)$ to cover two opposite edges of this rhombus. Then three new edges are added to reconnect both rotors; these edges have distance and angle $O(\varepsilon)$ from the long diagonal of the rhombus and the bisector of the smaller angle between the two great circles. The two fat triangles inside the rhombus are incorporated into one of the two rotors (the vertical red rotor in Figure 4.3); the two thin triangles near the diagonal are incorporated into both. Figure 4.3(b) shows a schematic of our overall construction.

Now let γ^* be a directed cycle in the dual graph Γ^* through the faces of one equatorial rotor. The corresponding polar region $P(\gamma^*)$ nearly fills a triangular region bounded by three bisector circles, each defined by an antipodal pair of crossing gadgets. This polar region completely covers one triangular face and nearly half of three square faces of Q. The reversal of γ^* defines an antipodally symmetric polar region.

Thus, the union of the polar regions defined by all four equatorial rotors covers the entire sphere except for a small "hole" near the center of each square face of Q, which we can make arbitrarily small by choosing ε appropriately. We cover these holes by adding a small rotor, reminiscent of the projection of a Schönhardt polyhedron, inside each square face of Q; see Figure 4.4. Finally, to complete the triangulation Γ, we arbitrarily triangulate the area between the rotors.

▶ **Theorem 4.3.** *There is a shortest-path triangulation of the sphere with no longitudinal shelling direction.*

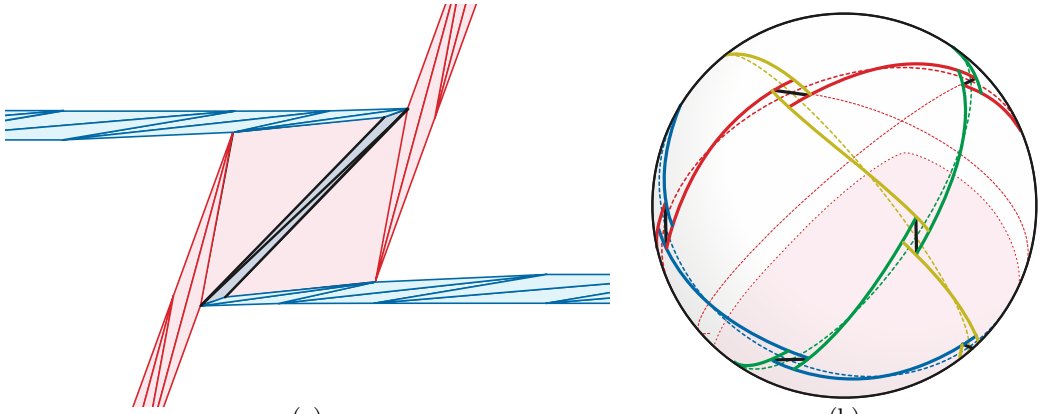

(a) (b)

Figure 4.3 (a) A single crossing gadget. (b) Constructing a totally unshellable triangulation. Each color of broken lines is an equatorial rotor; each short black line is the diagonal of a crossing gadget. The polar region of one (red) equatorial rotor is shaded.

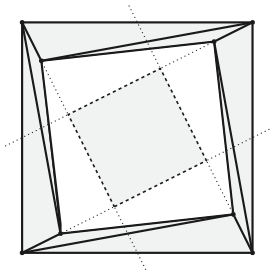

Figure 4.4 A square rotor (solid lines) and its polar region (dashed lines)

5 Sinking

Finally, we turn to an exact characterization of sinkable triangulations. Let Γ be our initial full shortest-path triangulation of the sphere. Lemma 2.2 implies that Γ is sinkable if and only if there is a weak triangulation Γ' that is θ-equivalent to Γ with all vertices below the equator.

Without loss of generality we can consider only weak embeddings Γ' where each vertex has the same x- and y-coordinates as in Γ. Let (x_i, y_i, z_i) and (x_i, y_i, z'_i) denote the coordinates of vertex i in Γ and Γ', respectively. Then Γ' is θ-equivalent to Γ if and only if $\text{vol}'(i,j,k) \geq 0$ for every non-polar face (i,j,k), where

$$\text{vol}'(i,j,k) := \det \begin{pmatrix} x_i & y_i & z'_i \\ x_j & y_j & z'_k \\ x_k & y_k & z'_k \end{pmatrix}$$

We reiterate that because we have fixed all x- and y-coordinates, the volume determinant $\text{vol}'(i,j,k)$ is a linear function of the vector z'.

▶ **Lemma 5.1.** *A spherical triangulation Γ is sinkable if and only if the following linear*

program is feasible:

$$\begin{array}{lrll} \textit{maximize} & \sum_i z'_i & & \\ \textit{subject to} & z'_i = -1 & \textit{for every vertex } i \textit{ of } f_{\mathsf{north}} & (5.1) \\ & \mathrm{vol}'(i,j,k) \geq 0 & \textit{for every non-polar face } (i,j,k) & \end{array}$$

Proof. Suppose $z' = (z'_1, \ldots, z'_n)$ is the z-coordinate vector of a weak triangulation Γ' that is θ-equivalent to Γ, such that $z'_i < 0$ for all i. We can move the vertices of north face of Γ' to the plane $z = -1$ by applying a linear transformation that preserves the z-axis and all longitudes. The coordinate vector of every other vertex i is a positive linear combination of the north-face coordiante vectors, so $z'_i < 0$ for all i. ◀

Lemma 5.1 immediately implies an algorithm to compute a sinking longitudinal morph, or report correctly that none exists, in weakly polynomial time, provided the input x- and y-coordinates are rational [42]. We obtain a simpler and faster algorithm (in the real RAM model) by identifying the optimal basis of the linear program, subject to a mild technical condition.

First we need a small extension of a result used in many planar morphing algorithms [21, 29, 49, 52, 53]. Let T be any straight-line plane graph whose outer face is a simple x-monotone polygon and whose inner faces are triangles. A weakly convex polygon W is *compatible* with T if there is a homeomorphism from boundary of T to the boundary of W that preserves x-coordinates. A weak planar triangulation T' is *x-equivalent* to T if it has the same underlying graph, every nondegenerate face of T' has the same orientation as the corresponding face of T, and corresponding vertices have equal x-coordinates.

▶ **Lemma 5.2.** *Given a triangulation T of an x-monotone polygon, and a weakly convex polygon W that is compatible with T, there is a weak planar triangulation T' that is x-equivalent to T and whose outer face is W.*

Proof sketch. If W is a strictly convex polygon, the lemma follows immediately from algorithms of Chrobak, Goodrich, Tammassia [21] and Kleist, Klemz, Lubiw, Schlipf, Staals, and Strash [52]; we extend these algorithms to weakly simple W using a limiting argument. See Appendix A for a complete proof. ◀

We emphasize that our algorithms never *compute* the weak triangulation T'; we only need to know that it exists.

▶ **Theorem 5.3.** *If $z' = (z'_1, \ldots, z'_n)$ is an optimal solution to linear program* (5.1)*, then z' is also a solution to the following $n \times n$ linear system:*

$$\begin{array}{rll} z'_i = -1 & \textit{for every vertex } i \textit{ of } f_{\mathsf{north}} & \\ \mathrm{vol}'(i,j,k) = 0 & \textit{for every down-face } (i,j,k) & (5.2) \end{array}$$

Proof. Let z' be any feasible solution for linear program (5.1), let Γ' be the corresponding southern weak embedding, and suppose that at least one down-face of Γ' is nondegenerate. We argue that we can construct another southern weak embedding Γ'' (that is, another feasible solution z'' to (5.1)) by increasing some z-coordinates and leaving all other coordinates fixed, which implies that z' is not an optimal solution to (5.1).

Call a vertex of Γ' *sober* if it is not incident to the north face or to any degenerate face. If any vertex of Γ' is sober, we can construct Γ'' by moving any sober vertex upward slightly and keeping all other vertices fixed. So without loss of generality, we assume that Γ' has no sober vertices.

We call a vertex i *upward-free* if i is not a vertex of the north face and $f_{\mathsf{above}}(i)$ is nondegenerate in Γ', *downward-free* if $f_{\mathsf{below}}(i)$ is nondegenerate in Γ', *totally free* if it is both upward- and downward-free, and *trapped* if $f_{\mathsf{above}}(i)$ and $f_{\mathsf{below}}(i)$ are both degenerate.

A *bar* in Γ' is a maximal circular arc that is covered by edges of Γ' and has no totally free vertices in its interior. Each bar is either a single edge or the union of one or more degenerate faces; in the latter case, the corresponding subset of faces in Γ are edge-connected, and their union is a θ-monotone disk. Equivalently, a nontrivial bar is the image in Γ' of a maximal edge-connected subset of faces of Γ that are all degenerate in Γ'. We call the subcomplex of Γ induced by these faces a *pre-bar*. The *endpoints* of a pre-bar are the preimages of the endpoints of its bar. Because no vertex of Γ' is sober, every vertex not incident to the north face is contained at least one bar.

Every upward-free vertex in Γ' is the image of a vertex on the northern boundary of a pre-bar in Γ. Every downward-free vertex in Γ' is either incident to the north face or the image of a vertex on the southern boundary of a pre-bar in Γ. The endpoints of a bar can be upward-free, downward-free, or both. Finally, each trapped vertex in Γ' is the image of a vertex in the interior of a pre-bar in Γ, and thus lies on a unique bar in Γ'.

We construct a new weak triangulation Γ'' by defining new coordinates $z''_i \geq z'_i$ for each vertex i. Let $\varepsilon > 0$ be any sufficiently small positive constant. Defining new coordinates for the free vertices of Γ' is straightforward:

- For every vertex i of the north face, we define $z''_i = z'_i$.
- For every upward-free vertex i, we define $z''_i = z'_i/(1+\varepsilon) > z'_i$.
- For every downward-free vertex i that is not also upward free, we define $z''_i = z'_i$.

Choosing sufficiently small ε already guarantees that any face that is non-degenerate in Γ' is also non-degenerate in Γ''. However, placing the trapped vertices to avoid inverting degenerate faces of Γ' requires more care.

Let β be any nontrivial bar in Γ', and let B be the corresponding pre-bar in Γ. We have already mapped the entire boundary of B to a spherical trapezoid τ in Γ''. Specifically, if β lies on the plane $z = ax + by$, then all upward-free vertices in β lie on the plane $z = (ax + by)/(1+\varepsilon)$ in Γ''.

Because β projects to a line segment in the plane $z = -1$, it lies inside an open hemisphere bounded by a *vertical* plane through the origin. Without loss of generality, suppose β lies in the hemisphere $y > 0$. Let π_y denote the function $(x, y, z) \mapsto (x/y, z/y)$; we can interpret this function geometrically as the gnomonic projection from S^2 to the plane $y = 1$. Then $\pi_y(\beta)$ is a non-vertical line segment, $\pi_y(B)$ is a triangulation of an x-monotone polygon, and $\pi_y(\tau)$ is a planar trapezoid whose lower boundary is a subset of $\pi_y(\beta)$ and whose upper boundary lies on a line parallel to $\pi_y(\beta)$. Each longitude ℓ through a trapped vertex i on β defines a *vertical* line $\pi_y(\ell)$ that must contain the point $(x_i/y_i, z''_i/y_i)$.

To summarize, $\pi_y(B)$ is a triangulation of an x-monotone polygon, and $\pi_y(\tau)$ is a weakly convex polygon that is compatible with $\pi_y(B)$. Thus, Lemma 5.2 implies that there is a weak triangulation $\pi_y(T'')$ that is x-equivalent to $\pi_y(B)$ and whose outer face is $\pi_y(\tau)$. Pulling $\pi_y(T'')$ back to the sphere gives is a weak triangulation T'' of the spherical trapezoid τ that is θ-equivalent to B. For each interior vertex i of B maps to a vertex in the closed interior of τ, which implies $z'_i \leq z''_i \leq z'_i/(1+\varepsilon)$.

We assemble the overall weak triangulation Γ'' by applying this construction to every bar in Γ'. (Processing each bar requires projecting to a different vertical tangent plane.) Because $z''_i \geq z'_i$ for every vertex i, and $z''_i > z'_i$ for at least one vertex i, the original weak triangulation Γ' cannot be an optimal solution to our linear program (5.1). ◀

▶ **Corollary 5.4.** *Given a shortest-path triangulation Γ of the sphere, we can either compute a longitudinal morph from Γ to a southern triangulation, or report correctly that no such morph exists, $O(n^{\omega/2})$ time, assuming linear system (5.2) is non-singular.*

Proof. The support of linear system (5.2) is precisely the planar graph $\Gamma^{\downarrow\swarrow}$. Thus, assuming the system is non-singular, it can be solved in $O(n^{\omega/2}) = O(n^{1.1864})$ time (in the real RAM model) via nested dissection and fast matrix multiplication [3, 55]. If the solution z' is a feasible point for linear program (5.1), the corresponding drawing Γ' is a weak southern triangulation longitudinally equivalent to Γ. If the system is non-singular, and the solution z' is not a feasible point for linear program (5.1), then by Theorem 5.3, we can correctly report that Γ is not sinkable. ◀

Theorem 5.3 is a strict generalization of the Awartani-Henderson embedding, described in the proof of Theorem 3.3. When Γ is shellable, its support graph $\Gamma^{\downarrow\swarrow}$ is acyclic. It follows that we can permute the rows and columns of the underlying matrix of (5.2) to obtain an upper-triangular matrix, which we can then solve by back-substitution. Each step of back-substitution assigns one z-coordinate, exactly mirroring one step of the Awartani-Henderson construction.

References

1. Hugo A. Akitaya, Radoslav Fulek, and Csaba D. Tóth. Recognizing weak embeddings of graphs. In *Proc. 29th Ann. ACM-SIAM Symp. Discrete Algorithms*, pages 274–292, 2018. doi:10.1137/1.9781611975031.20.
2. Soroush Alamdari, Patrizio Angelini, Fidel Barrera-Cruz, Timothy M. Chan, Giordano Da Lozzo, Giuseppe Di Battista, Fabrizio Frati, Penny Haxell, Anna Lubiw, Maurizio Patrignani, Vincenzo Roselli, Sahil Singla, and Bryan T. Wilkinson. How to morph planar graph drawings. *SIAM J. Comput.*, 46(2):824–852, 2017. doi:10.1137/16M1069171.
3. Noga Alon and Raphael Yuster. Matrix sparsification and nested dissection over arbitrary fields. *J. ACM*, 60(4):article 25, 18pp., 2013. doi:10.1145/2508028.2505989.
4. Marwan Awartani and David W. Henderson. Spaces of geodesic triangulations of the sphere. *Trans. Amer. Math. Soc.*, 304(2):721–732, 1987. doi:10.2307/2000738.
5. Fidel Barrera-Cruz, Penny Haxell, and Anna Lubiw. Morphing Schnyder drawings of planar triangulations. *Discrete Comput. Geom.*, 61(1):161–184, 2019. doi:10.1007/s00454-018-0018-9.
6. Therese Biedl, Anna Lubiw, and Jack Spalding-Jamieson. Morphing planar graph drawings via orthogonal box drawings. In *Proc. 32nd Int. Symp. Graph Drawing Network Vis.*, page to appear, 2024. doi:10.48550/arXiv.2409.04074.
7. Therese C. Biedl, Anna Lubiw, Mark Petrick, and Michael J. Spriggs. Morphing orthogonal planar graph drawings. *ACM Trans. Algorithms*, 9(4):29:1–29:24, 2013. doi:10.1145/2500118.
8. R. H. Bing and Michael Starbird. Linear isotopies in E^2. *Trans. Amer. Math. Soc.*, 237:205–222, 1978. doi:10.2307/1997619.
9. Ethan D. Bloch, Robert Connelly, and David W. Henderson. The space of simplexwise linear homeomorphisms of a convex 2-disk. *Topology*, 23(2):161–175, 1984. doi:10.1016/0040-9383(84)90037-5.
10. Gunnar Brinkmann. A simple and elementary proof of Whitney's unique embedding theorem. *Ars Math. Contemp.*, 20(2):195–197, 2021. doi:10.26493/1855-3974.2334.331.
11. Heinz Bruggesser and Peter Mani. Shellable decompositions of cells and spheres. *Math. Scand.*, 29:197–205, 1971. doi:10.7146/math.scand.a-11045.
12. Stewart S. Cairns. Deformations of plane rectilinear complexes. *Amer. Math. Monthly*, 51(5):247–252, 1944. doi:10.2307/2304300.

13 Stewart S. Cairns. Isotopic deformations of geodesic complexes on the 2-sphere and on the plane. *Ann. Math.*, 45(2):207–217, 1944. doi:10.2307/1969263.

14 Luca Castelli Aleardi, Olivier Devillers, and Éric Fusy. Canonical ordering for triangulations on the cylinder, with applications to periodic straight-line drawings. *J. Comput. Geom.*, 9(1):391–429, 2018. doi:10.20382/jocg.v9i1a14.

15 Augustin L. Cauchy. Recherches sur les polyèdres. *J. École Polytechnique*, 9(16):68–86, 1813. Presented February 1811. *Œuvres Complètes*, IIe Sèrie 1:7–25, 1905.

16 Frédéric Cazals and Sébastien Loriot. Computing the exact arrangement of circles on a sphere, with applications in structural biology: video. In *Proc. 23rd Ann. Symp. Comput. Geom.*, pages 119–120, 2007. doi:10.1145/1247069.1247088.

17 Frédéric Cazals and Sébastien Loriot. Computing the arrangement of circles on a sphere, with applications in structural biology. *Comput. Geom. Theory Appl.*, 42(6):551–565, 2009. doi:10.1016/j.comgeo.2008.10.004.

18 Jean Cerf. About the Bloch–Connelly–Henderson theorem on the simplexwise linear homeomorphisms of a convex 2-disk. Preprint, October 2019. doi:10.48550/arXiv.1910.00240.

19 Erin Wolf Chambers, Jeff Erickson, Patrick Lin, and Salman Parsa. How to morph graphs on the torus. In *Proc. 32nd Ann. ACM-SIAM Symp. Discrete Algorithms*, pages 2759–2778, 2021. doi:10.1137/1.9781611976465.164.

20 Bernard Chazelle, Leo J. Guibas, and D. T. Lee. The power of geometric duality. *BIT Numer. Math.*, 25(1):76–90, 1985. doi:10.1007/BF01934990.

21 Marek Chrobak, Michael T. Goodrich, and Roberto Tamassia. Convex drawings of graphs in two and three dimensions (preliminary version). In *Proc. 12th Ann. Symp. Comput. Geom.*, pages 319–328, 1996. doi:10.1145/237218.237401.

22 Yves Colin de Verdière. Sur un nouvel invariant des graphes et un critère de planarité. *J. Comb. Theory Ser. B*, 50(1):11–21, 1990. In French, English translation in [24]. doi:10.1016/0095-8956(90)90093-F.

23 Yves Colin de Verdière. Comment rendre géodésique une triangulation d'une surface? *L'Enseignment Mathématique*, 37:201–212, 1991. doi:10.5169/seals-58738.

24 Yves Colin de Verdière. On a new graph invariant and a criterion for planarity. In Neil Robertson and Paul Seymour, editors, *Graph Structure Theory*, number 147 in Contemporary Mathematics, pages 137–147. Amer. Math. Soc., 1993. English translation of [22] by Neil Calkin.

25 Robert Connelly, David W. Henderson, Chung-Wu Ho, and Michael Starbird. On the problems related to linear homeomorphisms, embeddings, and isotopies. In *Continua, Decompositions, Manifolds: Proc. Texas Topology Symposium, 1980*, pages 229–239. Univ. Texas Press, 1983.

26 Hubert de Fraysseix, János Pach, and Richard Pollack. How to draw a planar graph on a grid. *Combinatorica*, 10(1):41–51, 1990. doi:10.1007/BF02122694.

27 Krzysztof Diks and Piotr Sankowski. Dynamic plane transitive closure. In *Proc. 15th Ann. Europ. Symp. Algorithms*, number 4698 in Lecture Notes Comput. Sci., pages 594–604. Springer, 2007. doi:10.1007/978-3-540-75520-3_53.

28 Adrien Douady. Le shaddock á six becs. *Bull. APMEP*, 281:699–701, 1971. URL: https://www.apmep.fr/IMG/pdf/AAA71038.pdf.

29 Peter Eades, Qingwen Peng, Xuemin Lin, and Hiroshi Nagamochi. Straight-line drawing algorithms for hierarchical graphs and clustered graphs. *Algorithmica*, 44(1):1–32, 2006. doi:10.1007/s00453-004-1144-8.

30 Victor Eberhard. *Zur Morphologie der Polyeder*. Teubner, 1891.

31 Herbert Edelsbrunner and Leonidas J. Guibas. Topologically sweeping an arrangement. *J. Comput. Syst. Sci.*, 38(1):165–194, 1989. doi:10.1016/0022-0000(89)90038-X.

32 Herbert Edelsbrunner, Joseph O'Rourke, and Raimund Seidel. Constructing arrangements of lines and hyperplanes with applications. *SIAM Journal on Computing*, 15(2):341–363, 1986. doi:10.1137/0215024.

33 Jeff Erickson and Patrick Lin. Planar and toroidal morphs made easier. In *Proc. 29th Int. Symp. Graph Drawing Network Vis.*, number 12868 in Lecture Notes Comput. Sci., pages 123–137, 2021. doi:10.1007/978-3-030-92931-2_9.

34 Jeff Erickson and Patrick Lin. Planar and toroidal morphs made easier. *Journal of Graph Algorithms and Applications*, 27(2):95–118, 2023. doi:10.7155/jgaa.00616.

35 Cesim Erten, Stephen G. Kobourov, and Chandan Pitta. Intersection-free morphing of planar graphs. In Giuseppe Liotta, editor, *Proc. 11th Symp. Graph Drawing*, volume 2912 of *Lecture Notes Comput. Sci.*, pages 320–331. Springer, 2003. doi:10.1007/978-3-540-24595-7_30.

36 Michael S. Floater. Parametrization and smooth approximation of surface triangulations. *Comp. Aided Geom. Design*, 14(3):231–250, 1997. doi:10.1016/S0167-8396(96)00031-3.

37 Michael S. Floater. Parametric tilings and scattered data approximation. *Int. J. Shape Modeling*, 4(3–4):165–182, 1998. doi:10.1142/S021865439800012X.

38 Michael S. Floater and Craig Gotsman. How to morph tilings injectively. *J. Comput. Appl. Math.*, 101(1–2):117–129, 1999. doi:10.1016/S0377-0427(98)00202-7.

39 Radoslav Fulek and Jan Kyncl. Hanani-Tutte for approximating maps of graphs. In *Proc. 34th Int. Symp. Comput. Geom.*, number 99 in Leibniz Int. Proc. Informatics, pages 39:1–39:15. Schloss Dagstuhl–Leibniz-Zentrum für Informatik, 2018. doi:10.4230/LIPIcs.SoCG.2018.39.

40 Steven J. Gortler, Craig Gotsman, and Dylan Thurston. Discrete one-forms on meshes and applications to 3D mesh parameterization. *Comput. Aided Geom. Design*, 23(2):83–112, 2006. doi:10.1016/j.cagd.2005.05.002.

41 Craig Gotsman and Vitaly Surazhsky. Guaranteed intersection-free polygon morphing. *Computers & Graphics*, 25(1):67–75, 2001. doi:10.1016/S0097-8493(00)00108-4.

42 Martin Grötschel, László Lovász, and Alexander Schrijver. *Geometric Algorithms and Combinatorial Optimization*. Number 2 in Algorithms and Combinatorics. Springer-Verlag, 2nd edition, 1993.

43 Branko Grünbaum. Graphs of polyhedra; polyhedra as graphs. *Discrete Math.*, 307(3–5):445–463, 2007. doi:10.1016/j.disc.2005.09.037.

44 Joel Hass and Peter Scott. Simplicial energy and simplicial harmonic maps. *Asian J. Math.*, 19(4):593–636, 2015. doi:10.4310/AJM.2015.v19.n4.a2.

45 Chung-Wu Ho. On certain homotopy properties of some spaces of linear and piecewise linear homeomorphisms. I. *Trans. Amer. Math. Soc.*, 181:213–233, 1973. doi:10.2307/1996630.

46 Chung-Wu Ho. On certain homotopy properties of some spaces of linear and piecewise linear homeomorphisms. II. *Trans. Amer. Math. Soc.*, 181:235–243, 1973. doi:10.2307/1996631.

47 Chung-Wu Ho. Deforming P.L. homeomorphisms on a convex polygonal disk. *Pacific J. Math.*, 55(2):427–439, 1974. doi:10.2140/pjm.1974.55.427.

48 Seok-Hee Hong and Hiroshi Nagamochi. Convex drawings of hierarchical planar graphs and clustered planar graphs. *J. Discrete Algorithms*, 8(3):282–295, 2010. doi:10.1016/j.jda.2009.05.003.

49 John E. Hopcroft and Peter J. Kahn. A paradigm for robust geometric algorithms. *Algorithmica*, 7(1–6):339–380, 1992. doi:10.1007/BF01758769.

50 Borge Jessen. Orthogonal icosahedra. *Nordisk Matematisk Tidskrift*, 15(2/3):90–96, 1967. URL: https://www.jstor.org/stable/24524998.

51 Ming-Yang Kao. Linear-processor NC algorithms for planar directed graphs I: Strongly connected components. *SIAM J. Comput.*, 22(3):431–459, 1993. doi:10.1137/0222032.

52 Linda Kleist, Boris Klemz, Anna Lubiw, Lena Schlipf, Frank Staals, and Darren Strash. Convexity-increasing morphs of planar graphs. *Comput. Geom. Theory Appl.*, 84:69–88, 2019. doi:10.1016/j.comgeo.2019.07.007.

53 Boris Klemz. Convex drawings of hierarchical graphs in linear time, with applications to planar graph morphing. In *Proc. 29th Ann. Europ. Symp. Algorithms*, number 204 in Leibniz Int. Proc. Informatics, pages 57:1–57:15, 2021. doi:10.4230/LIPIcs.ESA.2021.57.

54 Stephen G. Kobourov and Matthew Landis. Morphing planar graphs in spherical space. *J. Graph Algorithms Appl.*, 12(1):113–127, 2006. doi:0.7155/jgaa.00162.

55 Richard J. Lipton, Donald J. Rose, and Robert Endre Tarjan. Generalized nested dissection. *SIAM J. Numer. Anal.*, 16:346–358, 1979. doi:10.1137/0716027.

56 Anna Lubiw and Mark Petrick. Morphing planar graph drawings with bent edges. *J. Graph Algorithms Appl.*, 15(2):205–227, 2011. doi:10.7155/jgaa.00223.

57 Yanwen Luo. Spaces of geodesic triangulations of surfaces. *Discrete Comput. Geom.*, 68(3):709–727, 2022. doi:10.1007/s00454-021-00359-4.

58 Yanwen Luo, Tianqi Wu, and Xiaoping Zhu. The deformation space of geodesic triangulations of flat tori. Preprint, July 2021. doi:10.48550/arXiv.2107.05159.

59 Yanwen Luo, Tianqi Wu, and Xiaoping Zhu. The deformation space of geodesic triangulations and generalized Tutte's embedding theorem. *Geom. Topol.*, 7:3361–3385, 2023. doi:10.2140/gt.2023.27.3361.

60 Yanwen Luo, Tianqi Wu, and Xiaoping Zhu. Spaces of geodesic triangulations are cells. Preprint, August 2024. doi:10.48550/arXiv.2204.10833.

61 Marc Noy. Acyclic and totally cyclic orientations in planar graphs. *Amer. Math. Monthly*, 108(1):66–68, 2001. doi:10.1080/00029890.2001.11919725.

62 Larry Palazzi and Jack Snoeyink. Counting and reporting red/blue segment intersections. *CVGIP: Graph. Models Image Proc.*, 56(4):304–310, 1994. doi:10.1006/cgip.1994.1027.

63 Jürgen Richter-Gebert. *Realization spaces of polytopes.* Number 1643 in Lecture Notes Math. Springer, 1996. doi:10.1007/BFb0093761.

64 Erich Schönhardt. Über die Zerlegung von Dreieckspolyedern in Tetraeder. *Math. Ann.*, 98(1):309–312, 1928. doi:10.1007/BF01451597.

65 Ernst Steinitz. Polyeder und Raumeinteilungen. *Enzyklopädie der mathematischen Wissenschaften mit Einschluss ihrer Anwendungen*, III.AB(12):1–139, 1916. URL: https://gdz.sub.uni-goettingen.de/id/PPN360609767.

66 Ernst Steinitz and Hans Rademacher. *Vorlesungen über die Theorie der Polyeder: unter Einschluß der Elemente der Topologie.* Number 41 in Grundlehren der mathematischen Wissenschaften. Springer-Verlag, 1934. Reprinted 1976. URL: http://eudml.org/doc/204064, doi:10.1007/978-3-642-65609-5.

67 Jorge Stolfi. Oriented projective geometry. In *Proc. 3rd Ann. Symp. Comput. Geom.*, pages 76–85, 1987. doi:10.1145/41958.41966.

68 Jorge Stolfi. *Primitives for Computational Geometry.* Ph.D. thesis, Dept. Comput. Sci., Stanford, May 1988. Reprinted as Technical Report SRC-RR-36, DEC / HP Labs Systems Research Center, January 1989. URL: https://shiftleft.com/mirrors/www.hpl.hp.com/techreports/Compaq-DEC/SRC-RR-36.pdf.

69 Jorge Stolfi. *Oriented Projective Geometry: A Framework for Geometric Computations.* Academic Press, New York, NY, 1991. doi:10.1016/C2013-0-11551-6.

70 Fred Supnick. On the perspective deformation of polyhedra. *Ann. Math.*, 49(3):714–730, 1948. doi:10.2307/1969055.

71 Fred Supnick. On the perspective deformation of polyhedra. II. Solution of the convexity problem. *Math. Ann.*, 53(2):551–555, 1951. doi:10.2307/1969572.

72 Vitaly Surazhsky and Craig Gotsman. Controllable morphing of compatible planar triangulations. *ACM Trans. Graphics*, 20(4):203–231, 2001. doi:10.1145/502783.502784.

73 Vitaly Surazhsky and Craig Gotsman. Morphing stick figures using optimal compatible triangulations. In *Proc. 9th Pacific Conf. Comput. Graphics Appl.*, pages 40–49, 2001. doi:10.1109/PCCGA.2001.962856.

74 Vitaly Surazhsky and Craig Gotsman. Intrinsic morphing of compatible triangulations. *Int. J. Shape Modeling*, 9(2):191–201, 2003. doi:10.1142/S0218654303000115.

75 Carsten Thomassen. Deformations of plane graphs. *J. Comb. Theory Ser. B*, 34(3):244–257, 1983. doi:10.1016/0095-8956(83)90038-2.

76 William T. Tutte. How to draw a graph. *Proc. London Math. Soc.*, 13(3):743–768, 1963. doi:10.1112/plms/s3-13.1.743.

77 Hassler Whitney. Congruent graphs and the connectivity of graphs. *Amer. J. Math.*, 54(1):150–168, 1932. doi:10.2307/2371086.

Appendix

A Omitted Proofs

▶ **Lemma 2.1.** *Any two θ-equivalent triangulations are connected by a longitudinal morph.*

Proof. Let Γ_0 and Γ_1 be two longitudinally equivalent embeddings of the same graph G. Without loss of generality (by scaling if necessary), each vertex has the same x- and y-coordinates in both embeddings. Let (x_i, y_i, z_i^0) and (x_i, y_i, z_i^1) denote the coordinate vectors of each vertex i in Γ_0 and Γ_1, respectively.

We define a longitudinal morph by linearly interpolating the z-coordinate of each vertex from z_i^0 to z_i^1. For each $t \in [0,1]$, let Γ_t denote the shortest-path *drawing* where each vertex i has coordinates $(x_i, y_i, (1-t)z_i^0 + t \cdot z_i^1)$. To complete the proof, it remains only to show that each drawing Γ_t is an embedding, or equivalently, that no face collapses to an arc during the morph.

For any three vertices i, j, k and any $t \in [0,1]$, let $\mathrm{vol}_t(i,j,k)$ denote the determinant

$$\det \begin{pmatrix} x_i & y_i & (1-t)\cdot z_i^0 + t \cdot z_i^1 \\ x_j & y_j & (1-t)\cdot z_i^0 + t \cdot z_i^1 \\ x_k & y_k & (1-t)\cdot z_i^0 + t \cdot z_i^1 \end{pmatrix}$$

This volume determinant is a linear function of t; specifically,

$$\mathrm{vol}_t(i,j,k) \;=\; (1-t)\cdot \mathrm{vol}_0(i,j,k) \;+\; t \cdot \mathrm{vol}_1(i,j,k).$$

Suppose i, j, k are the vertices of a *non-polar* face of Γ_0 in counterclockwise order, so that $\mathrm{vol}_0(i,j,k) > 0$. Because Γ_0 and Γ_1 are isomorphic, we have $\mathrm{vol}_1(i,j,k) > 0$; linearity immediately implies that $\mathrm{vol}_t(i,j,k) > 0$ for all $t \in [0,1]$.

Finally, for all t, the north pole lies in the interior of the north face of Γ_t, and the south pole lies in the interior of the south face of Γ_t. Thus, these faces may become (un)everted, but they always have non-empty interiors. ◀

▶ **Lemma 3.1.** *For every generic shortest-path triangulation Γ, the following conditions are equivalent:*

(a) *Γ is longitudinally shellable.*
(b) *$\Gamma^{\downarrow}$ is acyclic.*
(c) *$\Gamma^{\rightarrow}$ is strongly connected.*
(d) *$\Gamma^{\rightarrow}$ contains directed paths from f_{north} to f_{south} and from f_{south} to f_{north}.*
(e) *$\Gamma^{\searrow\swarrow}$ is acyclic.*

Proof. To prove (a)⇒(b), let $f_1, f_2, \ldots, f_{2n-4}$ be a longitudinal shelling of Γ, and consider any two faces f_k and f_l that share a common edge, where $k < l$. The disk U_k is θ-monotone, and therefore includes every point due north of f_k, but does not indlude f_l. It follows that f_l is south of f_k, and thus $\Gamma^{\downarrow}$ contains the directed edge $f_k \to f_l$. We conclude that $\Gamma^{\downarrow}$ is acyclic.

On the other hand, suppose $\Gamma^{\downarrow}$ is acyclic. Let $f_1, f_2, \ldots, f_{2n-4}$ be any topological ordering of $\Gamma^{\downarrow}$. Consider the prefix union $U_k = \bigcup_{i \le k} f_i$ for some index k, and suppose some longitude ℓ intersects two faces f_i and f_j such that $i \le k < j$. The intersection $\ell \cap f_i$ must be north of $\ell \cap f_j$, since otherwise $\Gamma^{\downarrow}$ would contain a path from f_i to f_j. Thus, U_k is a θ-monotone disk. It follows that $f_1, f_2, \ldots, f_{2n-4}$ is a longitudinal shelling of Γ.

The equivalence (b)⇔(c) follows from the duality between directed cycles and directed edge-cuts in directed planar graphs [51, 61].

The implication (c)⇒(d) is trivial. To prove the converse (c)⇐(d), suppose $\Gamma^{\rightarrow}$ contains directed paths $\pi_{\downarrow}$ from f_{north} to f_{south} and $\pi_{\uparrow}$ from from f_{south} to f_{north}. Consider an arbitrary vertex i. Because every edge in $\Gamma^{\rightarrow}$ is oriented from west to east, following edges of $\Gamma^{\rightarrow}$ starting at i must eventually reach some vertex of $\pi_{\downarrow}$. Thus, $\Gamma^{\rightarrow}$ contains a directed walk from i to f_{south}. Symmetrically, $\Gamma^{\rightarrow}$ contains a directed walk from f_{south} to i, starting with some prefix of $\pi_{\uparrow}$. We conclude that $\Gamma^{\rightarrow}$ is strongly connected.

The implication (b)⇒(e) is straightforward. If $i{\rightarrow}j$ is an edge of $\Gamma^{\searrow\swarrow}$, then $f_{\mathsf{above}}(i)$ is north of $f_{\mathsf{above}}(j)$, so there is a directed path from $f_{\mathsf{above}}(i)$ to $f_{\mathsf{above}}(j)$ in $\Gamma^{\downarrow}$. Thus, if $\Gamma^{\searrow\swarrow}$ contains a directed cycle, then $\Gamma^{\downarrow}$ also contains a directed cycle.

To complete the proof of the lemma, we prove the implication (e)⇒(b). Suppose $\Gamma^{\downarrow}$ contains a directed cycle. Let C be any strongly connected component of $\Gamma^{\downarrow}$ with more than one vertex, and let S denote the union of faces of Γ whose dual vertices are in C. The north and south faces are respectively the unique source and sink vertices of $\Gamma^{\downarrow}$, so they cannot be contained in C or in S. The following claims imply that S is a θ-monotone annulus that separates the polar faces of Γ.

▷ Claim A.1. *S intersects every longitude.*

Proof. Our proof of this claim adapts an argument of Palazzi and Snoeyink [62]. For any two faces f and f' in C, let $f \Downarrow f'$ indicate that some longitude ℓ intersects both f and f', and $f \cap \ell$ is north of $f' \cap \ell$. Let $f_1 \Downarrow f_2 \Downarrow \cdots \Downarrow f_r \Downarrow f_1$ be the minimum-length cycle through the faces in C with respect to this relation. We trivially have $r \geq 3$, since no face can be both north and south of another face. If any longitude does not intersect S, then some face f_i in this cycle is furthest east, which implies $f_{i-1} \Downarrow f_{i+1}$, contradicting the minimality of the cycle. ◁

▷ Claim A.2. *S is θ-monotone.*

Proof. Consider any longitude ℓ, and let a and b respectively denote the northernmost and southernmost point in $\ell \cap S$. Let $f'_a, f'_{a+1}, \ldots, f'_b$ denote the sequence of faces of Γ that intersect the longitudinal arc from a to b, in order from north to south; in particular, f'_a is the face of Γ just south of a, and f'_b is the face of Γ just north of b. We easily observe that $f'_a \in C$ and $f'_b \in C$, and that $\Gamma^{\downarrow}$ contains the edge $f'_i{\rightarrow}f'_{i+1}$ for each index $a \leq i < b$. It follows that all faces f'_i are in C, and therefore that $S \cap \ell$ is connected. ◁

It follows that S has two boundary curves, each of which is a simple θ-monotone cycle in Γ. Let σ denote the southern boundary of S. Any face f in S that is incident to σ has at least one out-neighbor in $\Gamma^{\downarrow}$ that is is not in C. On the other hand, because C is a strongly connected component of $\Gamma^{\downarrow}$, every face in S has at least one out-neighbor in $\Gamma^{\downarrow}$ that is in C. Thus, every edge of σ is a side of a *unique* down face; in particular, every edge of σ has a corresponding directed edge in $\Gamma^{\searrow\swarrow}$.

Finally, consider the set $\sigma^{\searrow\swarrow}$ of all such directed edges. If any two edges in $\sigma^{\searrow\swarrow}$ were directed toward each other, they would be the sides of a single down-face, which we just argued is impossible. Thus, $\sigma^{\searrow\swarrow}$ is a directed cycle in $\Gamma^{\searrow\swarrow}$. ◀

▶ **Theorem 3.3** (Awartani and Henderson [4]). *Every longitudinally shellable triangulation of the sphere is sinkable. Moreover, given any longitudinally shellable triangulation Γ, we can compute a longitudinal morph from Γ to a southern triangulation in $O(n)$ time.*

Proof. Let Γ be any longitudinally shellable triangulation. Lemma 2.2 implies that to prove the theorem, it suffices to construct a *weak* straight-line triangulation Γ' *in the plane* that is θ-equivalent to Γ, in $O(n)$ time. Here θ-equivalence means that each vertex of Γ' must lie on a particular ray from the origin. Because the edges of Γ' are straight line segments, our algorithm only needs to specify the location p'_i of each vertex i in Γ'.

Following Awartani and Henderson [4, Theorem 3.3], we construct Γ' by embedding the *faces* of Γ one at a time, following an arbitrary longitudinal shelling order $f_1, f_2, \ldots, f_{2n-4}$. Throughout the construction, we maintain a weakly convex polygon W that contains the origin in its interior. This region satisfies the following invariants for each vertex i, after faces $f_1, \ldots, f_k$ have been embedded:

- If $f_{\mathsf{above}}(i)$ has been embedded, then p'_i lies outside the interior of W.
- If in addition $f_{\mathsf{below}}(i)$ has *not* been embedded, then p'_i is a vertex of W.

To start the construction, we embed the north face f_1 by fixing its vertices *arbitrarily* on their respective rays. We also initialize W to be the convex hull of these three points. Then for each index k from 2 to $2n-5$, we proceed as follows:

- If f_i is an up-face, then all three vertices of f_k have already been placed on the boundary of W, so we embed f_k as the convex hull of its vertices. Because W is weakly convex, it contains the base segment of f_k. After embedding f_k, the apex of f_k is no longer a vertex of W, and the base of f_k becomes an edge of W. (The vertices of f_k may be collinear, in which case the interior of W does not change.)
- On the other hand, if f_k is a down-face, the base vertices of f_k have already been placed on the boundary of W, but not the apex. We place the apex of f_k at the intersection of its ray and the base of f_k; thus, f_k is embedded as a degenerate triangle. The apex of f_k becomes a new vertex of W, and the interior of W does not change.

In both cases, it is easy to verify that the invariants on W hold after f_k is embedded.

Finally, when we consider the south face f_{2n-4}, all of its vertices have already been placed. ◀

▶ **Lemma 5.2.** *Given a triangulation T of an x-monotone polygon, and a weakly convex polygon W that is compatible with T, there is a weak planar triangulation T' that is x-equivalent to T and whose outer face is W.*

Proof. When W is a *strictly* convex polygon, the lemma follows immediately from algorithms of Chrobak, Goodrich, Tammassia [21, Theorem 3.5] and Kleist, Klemz, Lubiw, Schlipf, Staals, and Strash [52, Lemma 11]. Both of these algorithms first compute positive weights $\lambda_{i\to j} > 0$ for each dart $i\to j$ of T so that the x-coordinate of each interior vertex j is the weighted average of the x-coordinates of the neighbors of j. For each interior vertex j, the incoming dart weights satisfy the constraints

$$x_j = \sum_i \lambda_{i\to j} x_i \quad \text{and} \quad \sum_i \lambda_{i\to j} = 1,$$

where for notational simplicity we define $\lambda_{i\to j} = 0$ if ij is not an edge of T. To compute the new embedding T', they fix the boundary vertices to the corresponding vertices of W, and then compute the interior y-coordinates by solving the linear system

$$y'_j = \sum_i \lambda_{i\to j} y'_j \qquad \text{for every interior vertex } j \tag{A.1}$$

Floater's extension [37] of Tutte's classical spring embedding theorem [76] guarantees that the resulting y-coordinates define a proper straight-line triangulation T'.

A straightforward limiting argument implies that when W is a *weakly* convex polygon, the drawing T' produced by either of these algorithms is a *weak* triangulation. Consider a continuous family $W(t)_{t\geq 0}$ of polygons, where $W(0) = W$ and $W(t)$ is strictly convex. For each $t \geq 0$, let $T'(t)$ denote the drawing computed by solving linear system (A.1); the linear system is always non-singular, so $T'(t)$ is well-defined and varies continuously with t. In particular, the signed area of each face of $T'(t)$ varies continuously with t and is positive for all $t > 0$. Thus, $T'(0)$ may contain degenerate faces, but no inverted faces. We conclude that $T' = T'(0)$ is a weak triangulation x-equivalent to T. ◀

B Experimental Results

We implemented a suite of algorithms to construct spherical triangulations, test shellability and sinkability, construct the Awartani-Henderson embeddings, and visualize longitudinal morphs. (This implementation was invaluable in identifying the objective function for our linear program (5.1) and leading us to conjecture Theorem 5.3.) In particular, to stress-test our algorithms, we implemented several randomized heuristics to construct "ugly" triangulations with long edges and skinny triangles, including generalizations of Schönhardt's polyhedron [64,70,71] and Jessen's icosahedra [50] (also known as "six-beaked shaddocks" [28]), convex hulls of random points, equatorial rotors, edge flipping and other refinement operations, and more severely, inserting arbitrary shortest paths as new edges.

We tested several thousand random triangulations, each with at least a hundred vertices. Without exception, every triangulation we generated had at least one *shellable* rotation, and for typical triangulations, even in the most pathological families we generated, we could find a shellable rotation by trying at most four random directions, and a sinkable rotation by trying at most three.

We systematically evaluated two families of random "ugly" triangulations. The first was generated by computing the convex hull of 100 random points on the unit sphere, and then attempting to perform a large number of edge flips, each replacing one edge separating a pair of facets whose union is convex. Specifically, for 10000 iterations, we chose a random edge and performed a flip if the union of its incident faces is convex; then for an additional 10000 iterations, we chose a random edge and performed a flip if the union of its incident faces is convex *and* the new edge is longer than the old edge. We generated 2231 triangulations in this family and tested 5000 random directions for each triangulation. On average, 66.0% of these random directions were shellable and 99.4% were sinkable; in the *worst* triangulation in this family,shown in Figure B.1, 17.8% of directions were shellable and 32.9% were sinkable.

Our second family was generated by starting with a regular tetrahedron and then adding shortest paths between 200 nearly antipodal points as edges. In each iteration, we chose two random unit vectors p and r, defined $q = -p + r/100$, removed all edges crossing the shortest path from p to q, inserted pq as an edge, and retriangulated the area around pq. We generated 1346 triangulations in this family and again tested 5000 random directions for each triangulation. On average, 32.6% of these random directions were shellable and 48.3% were sinkable; in the *worst* example in this family, shown in Figure B.2, 1.2% of directions were shellable and 1.4% were sinkable.

C Conjectures and Open Problems

The most obvious problem left open by our research is to prove or disprove Conjecture 2.3: Every shortest-path triangulation of the sphere has a sinkable rotation. More concretely, is

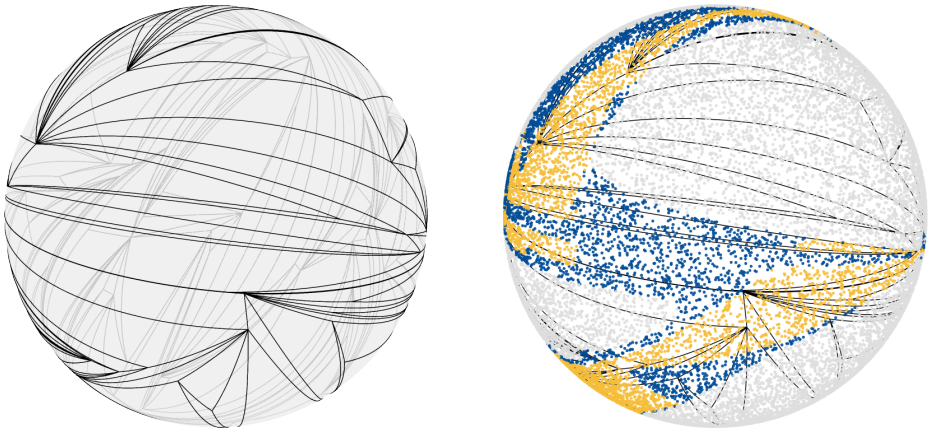

Figure B.1 Left: Our worst triangulation generated by randomly flipping edges, starting with the convex hull of random points. Right: Classifying random directions as shellable (yellow), not shellable but sinkable (blue), and not sinkable (light gray).

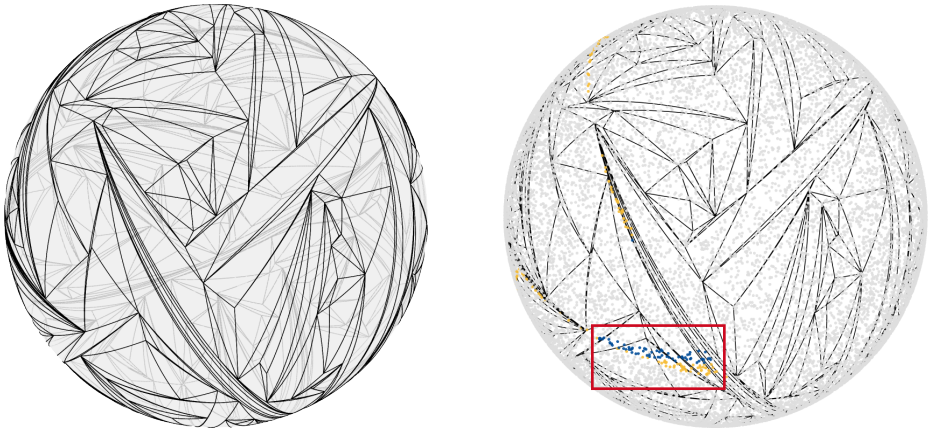

Figure B.2 Left: Our worst triangulation generated by forcing nearly antipodal edges. Right: Classifying random directions as shellable (yellow), not shellable but sinkable (blue), and not sinkable (light gray). Most visible shellable and sinkable directions are inside the red box.

there a polynomial-time algorithm that either finds a sinkable rotation of a given spherical triangulation or correctly reports that no such rotation exists?

Even much simpler questions about sinkability remain open. Experiments with thousands of random triangulations, similar to those reported in Appendix B, are consistent with the following conjectures:

▶ **Conjecture C.1.** *If every edge of a shortest-path triangulation* Γ *of the sphere has length at most* $\pi/2$*, then* Γ *(and therefore every rotation of* Γ*) is sinkable.*

▶ **Conjecture C.2.** *If no edge of a shortest-path triangulation* Γ *crosses the equator, then* Γ *is sinkable.*

Either Conjecture C.1 or Conjecture C.2 would imply an efficient morphing algorithm that introduces at most one *bend* into each edge. For example, Conjecture C.1 implies that if we subdivide each face of a triangulation Γ into four triangles, with new vertices at the midpoints of edges, the resulting triangulation Γ' is sinkable. Several authors have developed morphing algorithms for planar graphs that allow (or require) bends in intermediate edges [6, 7, 35, 56].

Conjecture C.2 would also imply that sinkability is *symmetric*, that is, a shortest-path triangulation can be longitudinally morphed into the southern hemisphere if and only if it can be longitudinally morphed into the northern hemisphere. The corresponding claim about longitudinal shellability follows trivially from Lemma 3.1; for any unit vector p, the graph $\Gamma^{\downarrow}(p)$ is the reversal of $\Gamma^{\downarrow}(-p)$, and the reversal of a directed acyclic graph is a directed acyclic graph.

A fast algorithm to find sinkable rotations would imply an efficient spherical morphing algorithm, but the resulting morphs have one undesirable feature: Even when we are morphing between full triangulations, some intermediate triangulations are not full. In contrast, Cairns's edge-collapsing argument actually yields morphs in which every triangulation is full. We conjecture that techniques used to efficiently construct piecewise-linear planar morphs, which are based on Cairns's strategy, can be generalized to the sphere to yield *full* morphs.

Using Cairns's result, Ho [45,46] proved that the space of all embeddings of maximal planar graphs, with a given outer triangular face, is topologically trivial, Ho's result was generalized to planar triangulations with convex outer faces by Bloch, Connelly, and Henderson [9]; more recent proofs have been given by Cerf [18] and Luo [57]. Connelly, Henderson, Ho, and Starbird [25] conjectured that every isotopy class of geodesic triangulations on *any* surface S with constant curvature is homotopy-equivalent to the group $Isom_0(S)$ of isometries of S that are homotopic to the identity. Their conjecture was recently proved both for the flat torus [34, 58] and for arbtriary negative-curvature surfaces [59]; all of these proofs rely on nontrivial extensions of Floater's theorem [23, 40, 44, 59]. The only closed surface for which this conjecture remains open is the sphere!

Finally, we remark in passing that essentially nothing is known about morphing the more general class of *long geodesic embeddings*, whose edges are great-circular arcs that may be longer than a semicircle. Even representing such embeddings is nontrivial; in particular, vertex coordinates and a rotation system do not necessarily specify a unique long geodesic embedding. Using ad-hoc arguments, we have been able to prove that any two long geodesic embeddings of K_4 are connected by a continuous family of such embeddings. Do such morphs exist for all planar graphs? Can they be constructed efficiently?